



# LiDAR Remote Sensing Data Collection: Mt. St. Helens, WA

January 15th, 2010

Submitted to:

Scott Smith  
David C. Smith & Associates  
1734 SE Tacoma St.  
Portland, OR 97202

Submitted by:

Watershed Sciences  
257B SW Madison Ave.  
Corvallis, OR 97333

529 SW 3rd Ave. Suite 300  
Portland, Oregon 97204



# LiDAR Remote Sensing Data Collection: Mt. St. Helens, WA

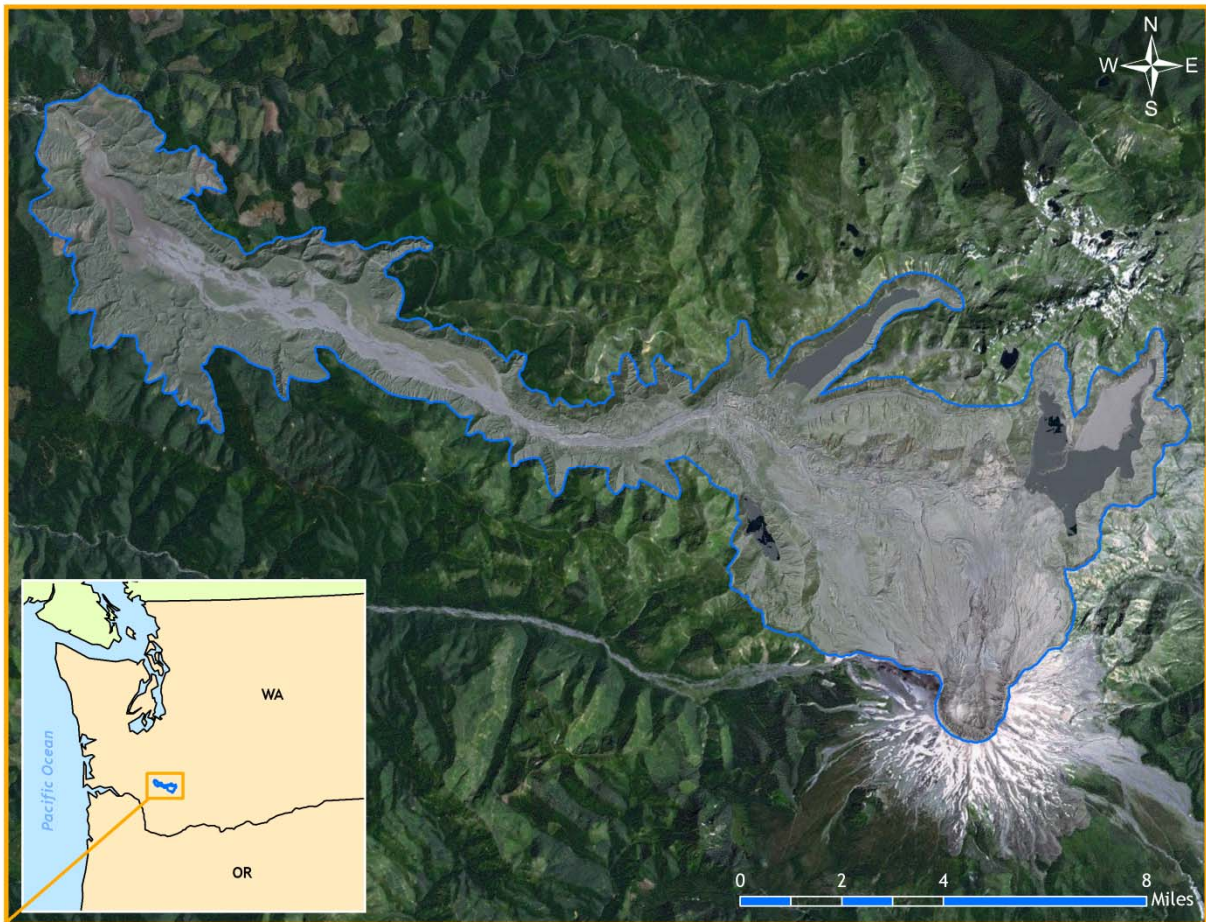
## TABLE OF CONTENTS

1. Overview .....	1
2. Acquisition .....	2
2.1 Airborne Survey - Instrumentation and Methods .....	2
2.2 Ground Survey - Instrumentation and Methods.....	3
2.2.1 Survey Control.....	3
2.2.2 RTK Survey.....	3
3. Data Processing .....	5
3.1 Applications and Work Flow Overview .....	5
3.2 Aircraft Kinematic GPS and IMU Data .....	5
3.3 Laser Point Processing.....	6
4. LiDAR Accuracy Assessment .....	7
4.1 Laser Noise and Relative Accuracy .....	7
4.2 Absolute Accuracy .....	8
5. Study Area Results.....	9
5.1 Data Summary .....	9
5.2 Data Density/Resolution .....	9
5.3 Relative Accuracy Calibration Results .....	12
5.4 Absolute Accuracy .....	12
5.5 Projection/Datum and Units .....	14
6. Deliverables .....	14
7. Selected Images .....	16
8. Glossary .....	22
9. Citations .....	22
Appendix A.....	23

# 1. Overview

Watershed Sciences, Inc. (WS) collected Light Detection and Ranging (LiDAR) data of the Mt. St. Helens study area (Mt. St. Helens NVM and the upper Toutle River), WA on September 16th - 20th, 2009. The total area of delivered LiDAR for the Mt. St. Helens area of interest (AOI) is 52,838 acres (**Figure 1**). The requested area was expanded to include a 100 m buffer to ensure complete coverage and adequate point densities around survey area boundaries.

*Figure 1. Mt. St. Helens, WA AOI (background image from <http://services.arcgisonline.com/v92>).*



## 2. Acquisition

### 2.1 Airborne Survey - Instrumentation and Methods

The LiDAR survey uses a Leica ALS50 and ALS60 Phase II laser system. The majority of the Mt. St. Helens survey was conducted at an above ground altitude of 1300m with sensor scan angles of  $\pm 13^\circ$  from nadir<sup>1</sup> yielding an approximate swath width of 600m. The St Helens crater and rim were surveyed at an above ground altitude of 1400m with sensor scan angles of  $\pm 12^\circ$  from nadir, yielding an approximate swath width of 595m.

The survey pulse rate was designed to yield an average native density (number of pulses emitted by the laser system) of  $\geq 8$  points per square meter over terrestrial surfaces. It is not uncommon for some types of surfaces (e.g. dense vegetation or water) to return fewer pulses than the laser originally emitted. These discrepancies between ‘native’ and ‘delivered’ density will vary depending on terrain, land cover and the prevalence of water bodies. All survey areas were surveyed with an opposing flight line side-lap of  $\geq 50\%$  ( $\geq 100\%$  overlap) to reduce laser shadowing and increase surface laser painting.

The Leica ALS50 and ALS60 Phase II systems allows up to four range measurements (returns) per pulse, and all discernable laser returns were processed for the output dataset. For this survey, the diameter of the individual laser pulse on the ground at nadir is 30-32cm.



The Cessna Caravan is a stable platform, ideal for flying slow and low for high density projects. The Leica ALS50 sensor head installed in the Caravan is shown on the left.

To accurately solve for laser point position (geographic coordinates x, y, z), the positional coordinates of the airborne sensor and the attitude of the aircraft were recorded continuously throughout the LiDAR data collection mission. Aircraft position was measured twice per second (2 Hz) by an onboard differential GPS unit. Aircraft attitude was measured 200 times per second (200 Hz) as pitch, roll and yaw (heading) from an onboard inertial measurement

---

<sup>1</sup> Nadir refers to the perpendicular vector to the ground directly below the aircraft. Nadir is commonly used to measure the angle from the vector and is referred to a “degrees from nadir”.

unit (IMU). To allow for post-processing correction and calibration, aircraft/sensor position and attitude data are indexed by GPS time.

## 2.2 Ground Survey - Instrumentation and Methods

The following ground survey data were collected to enable the geo-spatial correction of the aircraft positional coordinate data collected throughout the flight, and to allow for quality assurance checks on final LiDAR data products.

### 2.2.1 Survey Control

Multiple static (1 Hz recording frequency) ground surveys are conducted over monuments with known coordinates concurrently with the airborne data collection. (Table 1, Figure 2). Indexed by time, these GPS data are used to correct the continuous onboard measurements of aircraft position recorded throughout the mission. Multiple sessions were processed over the same monument to confirm antenna height measurements and reported position accuracy. After the airborne survey, these static GPS data were then processed using triangulation with Continuously Operating Reference Stations (CORS) stations, and checked against the Online Positioning User Service (OPUS) to quantify daily variance. Controls were located within 13 nautical miles of the mission area(s).



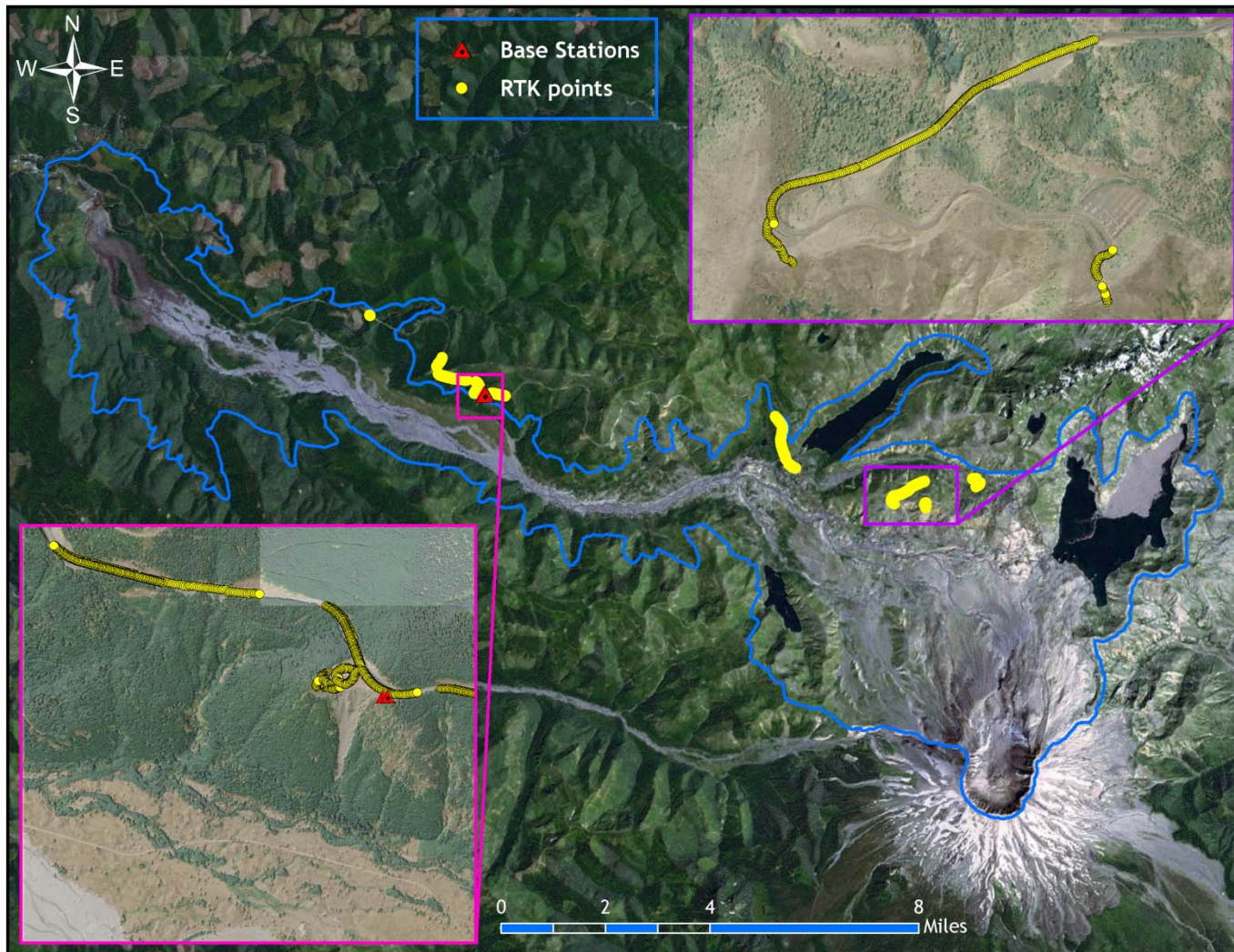
Table 1. Base Station Survey Control coordinates for the entire Mt. St. Helens survey area.

Base Station ID	Datum: NAD83 (CORS91)		GRS80
	Latitude	Longitude	Ellipsoid Z (meters)
HELCH4	46° 18' 27.67034"	122° 23' 35.79824"	796.214
HELCH3	46° 18' 27.68031"	122° 23' 34.88857"	797.143

### 2.2.2 RTK Survey

To enable assessment of LiDAR data accuracy, ground truth points were collected using GPS based real-time kinematic (RTK) surveying. For an RTK survey, the ground crew uses a roving unit to receive radio-relayed corrected positional coordinates for all ground points from a GPS base station set up over a survey control monument. Instrumentation includes multiple Trimble DGPS units (R8). RTK surveying allows for precise location measurements with an error ( $\sigma$ ) of  $\leq 1.5$  cm (0.6 in). Due to access constraints to suitable hard-surface roads within the survey area, it was necessary to collect RTK points on a road immediately adjacent to the site (Figure 2). The LiDAR survey was expanded to cover the area along Spirit Lake Hwy. allowing for adjacent RTK points to be used in calibration and accuracy assessment. Figure 2 below portrays a distribution of RTK point locations used for the survey areas.

Figure 2. RTK and base station locations used for the Mt. St. Helens AOI (background image from <http://services.arcgisonline.com/v92>). Inset images were made from 3-ft LiDAR derived highest hit models and NAIP orthoimagery.



## 3. Data Processing

### 3.1 Applications and Work Flow Overview

1. Resolved kinematic corrections for aircraft position data using kinematic aircraft GPS and static ground GPS data.  
**Software:** Waypoint GPS v.8.10, Trimble Geomatics Office v.1.62
2. Developed a smoothed best estimate of trajectory (SBET) file that blends post-processed aircraft position with attitude data. Sensor head position and attitude were calculated throughout the survey. The SBET data were used extensively for laser point processing.  
**Software:** IPAS v.1.4
3. Calculated laser point position by associating SBET position to each laser point return time, scan angle, intensity, etc. Created raw laser point cloud data for the entire survey in \*.las (ASPRS v1.2) format.  
**Software:** ALS Post Processing Software v.2.69
4. Imported raw laser points into manageable blocks (less than 500 MB) to perform manual relative accuracy calibration and filter for pits/birds. Ground points were then classified for individual flight lines (to be used for relative accuracy testing and calibration).  
**Software:** TerraScan v.9.017
5. Using ground classified points per each flight line, the relative accuracy was tested. Automated line-to-line calibrations were then performed for system attitude parameters (pitch, roll, heading), mirror flex (scale) and GPS/IMU drift. Calibrations were performed on ground classified points from paired flight lines. Every flight line was used for relative accuracy calibration.  
**Software:** TerraMatch v.9.004
6. Position and attitude data were imported. Resulting data were classified as ground and non-ground points. Statistical absolute accuracy was assessed via direct comparisons of ground classified points to ground RTK survey data. Data were then converted to orthometric elevations (NAVD88) by applying a Geoid03 correction. Ground models were created as a triangulated surface and exported as ArcInfo ASCII grids at a 1 m pixel resolution.  
**Software:** TerraScan v.9.017, ArcMap v.9.3.1, TerraModeler v.9.003

### 3.2 Aircraft Kinematic GPS and IMU Data

LiDAR survey datasets were referenced to the 1 Hz static ground GPS data collected over pre-surveyed monuments with known coordinates. While surveying, the aircraft collected 2 Hz kinematic GPS data, and the onboard inertial measurement unit (IMU) collected 200 Hz aircraft attitude data. Waypoint GPS v.8.10 was used to process the kinematic corrections for the aircraft. The static and kinematic GPS data were then post-processed after the survey to obtain an accurate GPS solution and aircraft positions. IPAS v.1.4 was used to develop a trajectory file that includes corrected aircraft position and attitude information. The trajectory data for the entire flight survey session were incorporated into a final smoothed best estimated trajectory (SBET) file that contains accurate and continuous aircraft positions and attitudes.



### 3.3 Laser Point Processing

Laser point coordinates were computed using the IPAS and ALS Post Processor software suites based on independent data from the LiDAR system (pulse time, scan angle), and aircraft trajectory data (SBET). Laser point returns (first through fourth) were assigned an associated (x, y, z) coordinate along with unique intensity values (0-255). The data were output into large LAS v. 1.2 files; each point maintains the corresponding scan angle, return number (echo), intensity, and x, y, z (easting, northing, and elevation) information.

These initial laser point files were too large for subsequent processing. To facilitate laser point processing, bins (polygons) were created to divide the dataset into manageable sizes (< 500 MB). Flightlines and LiDAR data were then reviewed to ensure complete coverage of the survey area and positional accuracy of the laser points.

Laser point data were imported into processing bins in TerraScan, and manual calibration was performed to assess the system offsets for pitch, roll, heading and scale (mirror flex). Using a geometric relationship developed by Watershed Sciences, each of these offsets was resolved and corrected if necessary.

LiDAR points were filtered for noise, pits (artificial low points), and birds (true birds as well as erroneously high points) by screening for absolute elevation limits, isolated points and height above ground. Each bin was then manually inspected for remaining pits and birds and spurious points were removed. In a bin containing approximately 7.5-9.0 million points, an average of 50-100 points are typically found to be artificially low or high. Common sources of non-terrestrial returns are clouds, birds, vapor, haze, decks, brush piles, etc.

Internal calibration was refined using TerraMatch. Points from overlapping lines were tested for internal consistency and final adjustments were made for system misalignments (i.e., pitch, roll, heading offsets and scale). Automated sensor attitude and scale corrections yielded 3-5 cm improvements in the relative accuracy. Once system misalignments were corrected, vertical GPS drift was then resolved and removed per flight line, yielding a slight improvement (<1 cm) in relative accuracy.

The TerraScan software suite is designed specifically for classifying near-ground points (Soininen, 2004). The processing sequence began by 'removing' all points that were not 'near' the earth based on geometric constraints used to evaluate multi-return points. The resulting bare earth (ground) model was visually inspected and additional ground point modeling was performed in site-specific areas to improve ground detail. This manual editing of grounds often occurs in areas with known ground modeling deficiencies, such as: bedrock outcrops, cliffs, deeply incised stream banks, and dense vegetation. In some cases, automated ground point classification erroneously included known vegetation (i.e., understory, low/dense shrubs, etc.). These points were manually reclassified as non-grounds. Ground surface rasters were developed from triangulated irregular networks (TINs) of ground points.

## 4. LiDAR Accuracy Assessment

Our LiDAR quality assurance process uses the data from the real-time kinematic (RTK) ground survey conducted in the survey area. In this project, a total of 1468 RTK GPS measurements were collected on hard surfaces distributed among multiple flight swaths. To assess absolute accuracy, we compared the location coordinates of these known RTK ground survey points to those calculated for the closest laser points.

### 4.1 Laser Noise and Relative Accuracy

Laser point absolute accuracy is largely a function of laser noise and relative accuracy. To minimize these contributions to absolute error, we first performed a number of noise filtering and calibration procedures prior to evaluating absolute accuracy.

#### *Laser Noise*

For any given target, laser noise is the breadth of the data cloud per laser return (i.e., last, first, etc.). Lower intensity surfaces (roads, rooftops, still/calm water) experience higher laser noise. The laser noise range for this survey was approximately 0.02 meters.

#### *Relative Accuracy*

Relative accuracy refers to the internal consistency of the data set - the ability to place a laser point in the same location over multiple flight lines, GPS conditions, and aircraft attitudes. Affected by system attitude offsets, scale, and GPS/IMU drift, internal consistency is measured as the divergence between points from different flight lines within an overlapping area. Divergence is most apparent when flight lines are opposing. When the LiDAR system is well calibrated, the line-to-line divergence is low (<10 cm). See Appendix A for further information on sources of error and operational measures that can be taken to improve relative accuracy.

### Relative Accuracy Calibration Methodology

1. Manual System Calibration: Calibration procedures for each mission require solving geometric relationships that relate measured swath-to-swath deviations to misalignments of system attitude parameters. Corrected scale, pitch, roll and heading offsets were calculated and applied to resolve misalignments. The raw divergence between lines was computed after the manual calibration was completed and reported for each survey area.
2. Automated Attitude Calibration: All data were tested and calibrated using TerraMatch automated sampling routines. Ground points were classified for each individual flight line and used for line-to-line testing. System misalignment offsets (pitch, roll and heading) and scale were solved for each individual mission and applied to respective mission datasets. The data from each mission were then blended when imported together to form the entire area of interest.
3. Automated Z Calibration: Ground points per line were utilized to calculate the vertical divergence between lines caused by vertical GPS drift. Automated Z calibration was the final step employed for relative accuracy calibration.

## 4.2 Absolute Accuracy

The vertical accuracy of the LiDAR data is described as the mean and standard deviation (sigma -  $\sigma$ ) of divergence of LiDAR point coordinates from RTK ground survey point coordinates. To provide a sense of the model predictive power of the dataset, the root mean square error (RMSE) for vertical accuracy is also provided. These statistics assume the error distributions for x, y, and z are normally distributed, thus we also consider the skew and kurtosis of distributions when evaluating error statistics.

Statements of statistical accuracy apply to fixed terrestrial surfaces only and may not be applied to areas of dense vegetation or steep terrain. To calibrate laser accuracy for the LiDAR dataset, 1468 RTK ground survey points were collected on fixed, hard-packed road surfaces within the survey area.

## 5. Study Area Results

Summary statistics for point resolution and accuracy (relative and absolute) of the LiDAR data collected in the Mt. St. Helens survey area are presented below in terms of central tendency, variation around the mean, and the spatial distribution of the data (for point resolution by bin or processing tile).

### 5.1 Data Summary

*Table 2. Resolution and Accuracy - Specifications and Achieved Values.*

	Targeted	Achieved
Resolution:	$\geq 8$ points/m <sup>2</sup>	0.88 points/ft <sup>2</sup> (9.45 points/m <sup>2</sup> )
Vertical Accuracy (1 $\sigma$ ):	<13 cm	0.11 ft (3.2 cm)

### 5.2 Data Density/Resolution

The average data density across the survey exceeds the targeted resolution (**Table 2**). This high resolution is due to conservative flight planning to ensure targeted densities in the varied terrain of the Mt. St. Helens survey area. However, it is not uncommon for some types of surfaces (e.g. dense vegetation, agricultural fields, and water) to return fewer pulses than the laser originally emitted. These discrepancies between ‘native’ and ‘delivered’ density will vary depending on terrain, land cover and the prevalence of water bodies.

Ground classifications were derived from automated ground surface modeling and manual, supervised classifications where it was determined that the automated model had failed. Ground-classified return densities will be lower in areas of dense vegetation, water, or buildings.

The maps in **Figure 5** identify the average native and ground point densities for each processing bin.

LiDAR data resolution for the Mt. St. Helens survey area:

- Average Point (First Return) Density = 0.88 points/ft<sup>2</sup> (9.45 points/m<sup>2</sup>)
- Average Ground Point Density = 0.32 points/ft<sup>2</sup> (3.47 points/m<sup>2</sup>)

Figure 3. Density distribution for first return laser points.

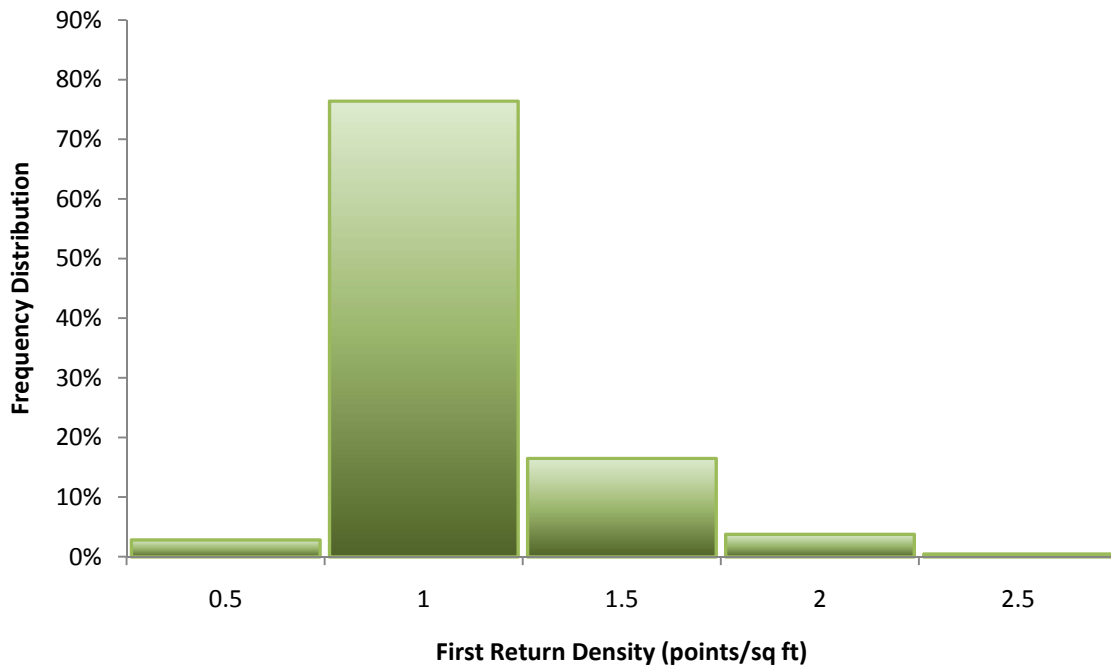


Figure 4. Density distribution for ground-classified laser points.

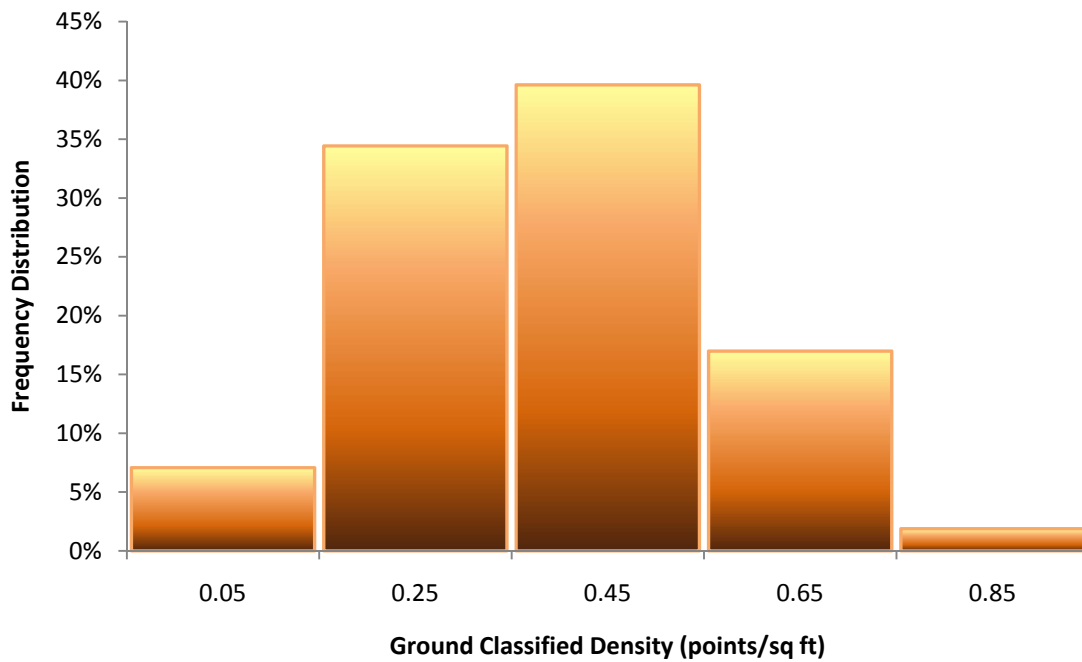
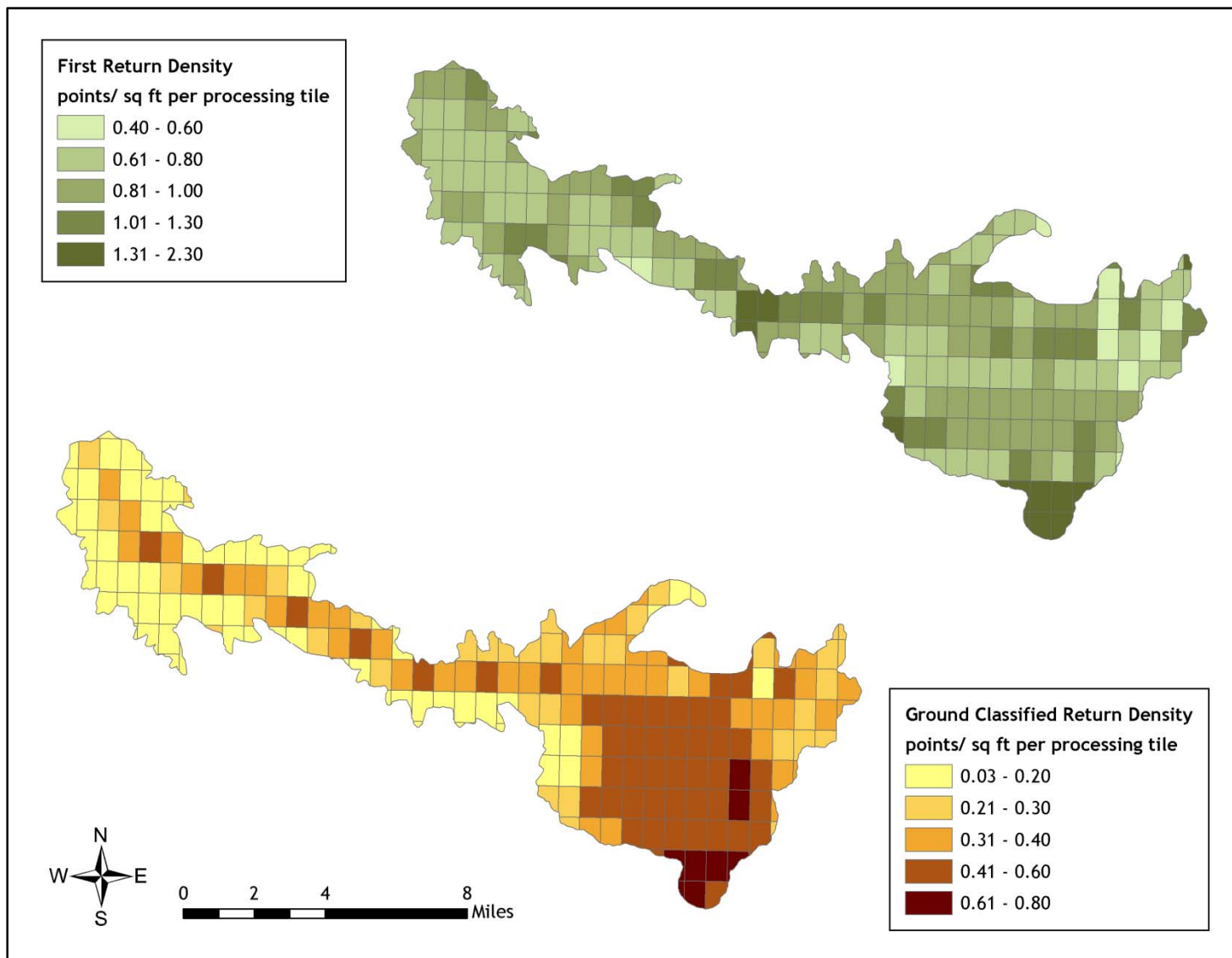


Figure 5. First return and ground-classified laser point data density per USGS 1/100th quadrangle

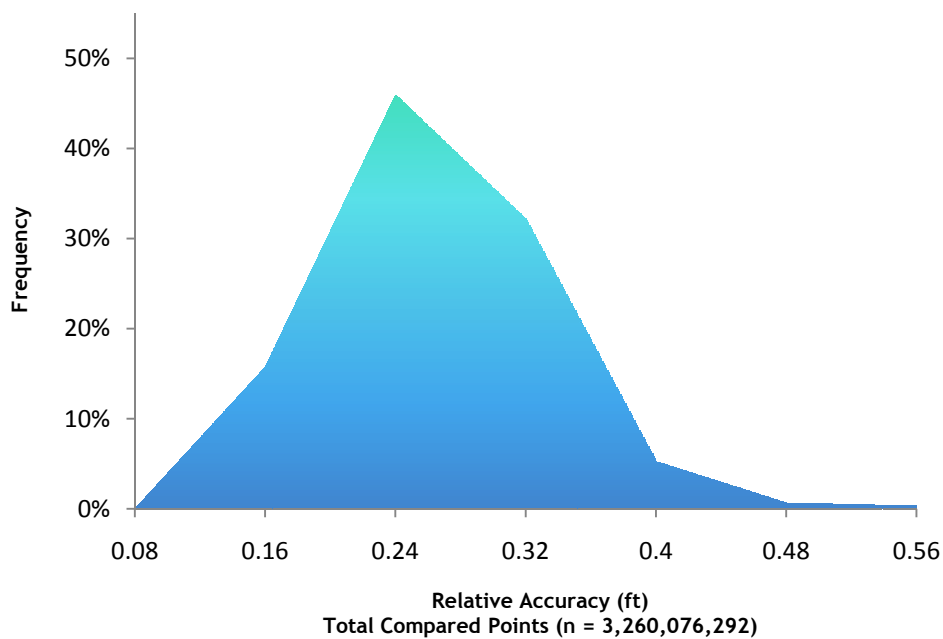


### 5.3 Relative Accuracy Calibration Results

Relative accuracies for the Mt. St. Helens survey area measure the full survey calibration including areas outside the delivered boundary.

- Project Average = 0.189 ft (0.058 m)
- Median Relative Accuracy = 0.209 ft (0.064 m)
- 1 $\sigma$  Relative Accuracy = 0.246 ft (0.075 m)
- 2 $\sigma$  Relative Accuracy = 0.329 ft (0.100 m)

Figure 6. Distribution of relative accuracies per flight line, non slope-adjusted.



### 5.4 Absolute Accuracy

Absolute accuracies for the Mt. St. Helens survey area

Table 3. Absolute Accuracy - Deviation between laser points and RTK hard surface survey points.

RTK Survey Sample Size (n): 1468			
Root Mean Square Error (RMSE) = 0.115 ft (0.035 m)		Minimum $\Delta z$ = -0.341 ft (-0.104 m)	
Standard Deviations		Maximum $\Delta z$ = 0.505 ft (0.154 m)	
1 sigma ( $\sigma$ ) =	0.105 ft (0.032 m)	2 sigma ( $\sigma$ ) =	0.233 ft (0.071 m)
		Average $\Delta z$ = 0.013 ft (0.004 m)	

Figure7. Absolute Accuracy - Histogram Statistics, based on 1468 hard surface points.

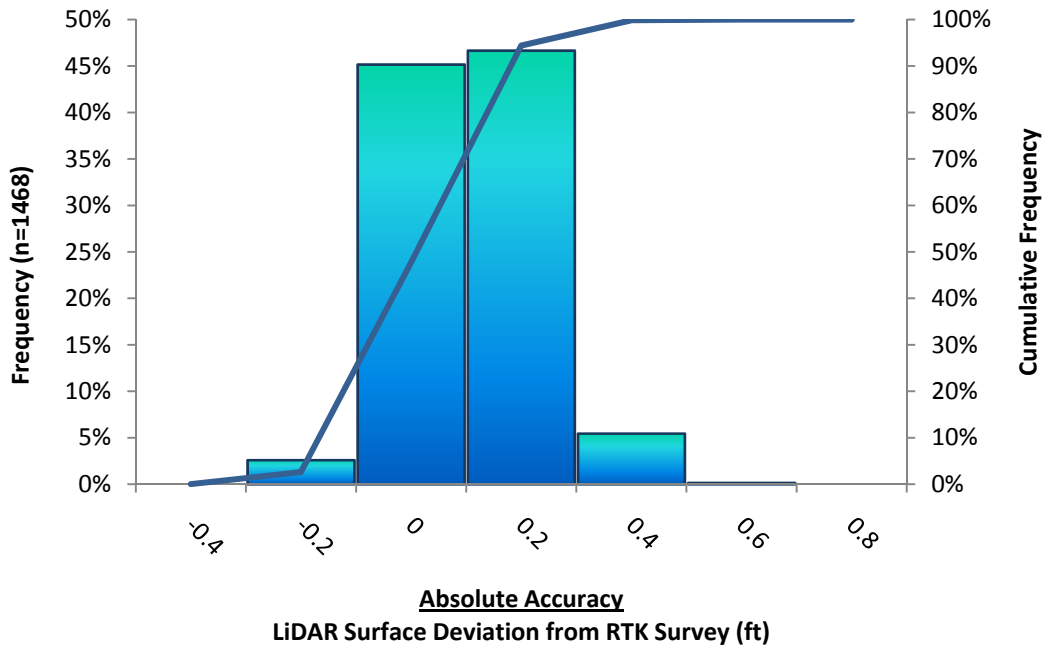
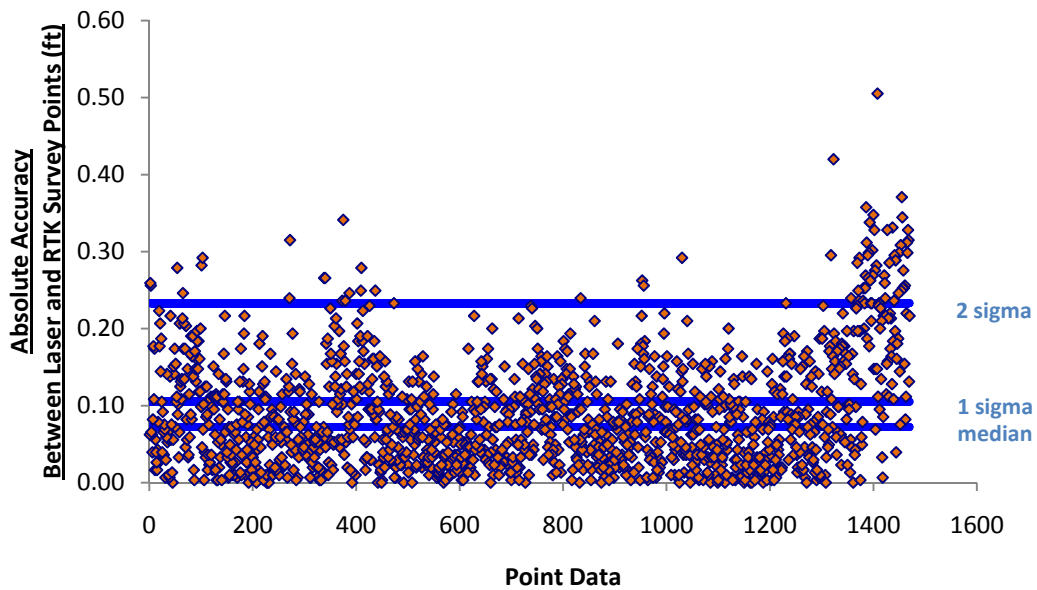


Figure8. Absolute Accuracy - Absolute Deviation, based on 1468 hard surface points.





## 5.5 Projection/Datum and Units

Projection:		Washington State Plane South
Datum	Vertical:	NAVD88 Geoid03
	Horizontal:	NAD83
Units:		U.S. Survey Feet

## 6. Deliverables

Point Data:	<ul style="list-style-type: none"> <li>All laser returns (LAS v. 1.2 format; 1/100th USGS quad delineation)</li> </ul>
Vector Data:	<ul style="list-style-type: none"> <li>LiDAR index (shapefile format; 1/100<sup>th</sup> USGS quad delineation)</li> <li>Raster index (shapefile format; 1/4<sup>th</sup> USGS quad delineation)</li> <li>SBET Trajectories (shapefile format)</li> </ul>
Raster Data:	<ul style="list-style-type: none"> <li>Elevation models of entire AOI (1-m resolution): <ul style="list-style-type: none"> <li>Bare Earth Model (ESRI GRID format; 1/4<sup>th</sup> USGS quad delineation)</li> <li>Highest Hit Model (ESRI GRID format; 1/4<sup>th</sup> USGS quad delineation)</li> </ul> </li> <li>Intensity images (GeoTIFF format, .5-m resolution, 1/100th USGS quad delineation)</li> </ul>
Data Report:	<ul style="list-style-type: none"> <li>Full report containing introduction, methodology, and accuracy</li> </ul>

Point Data (per 1/100th USGS Quad delineation\*)  
 LAS v1.2

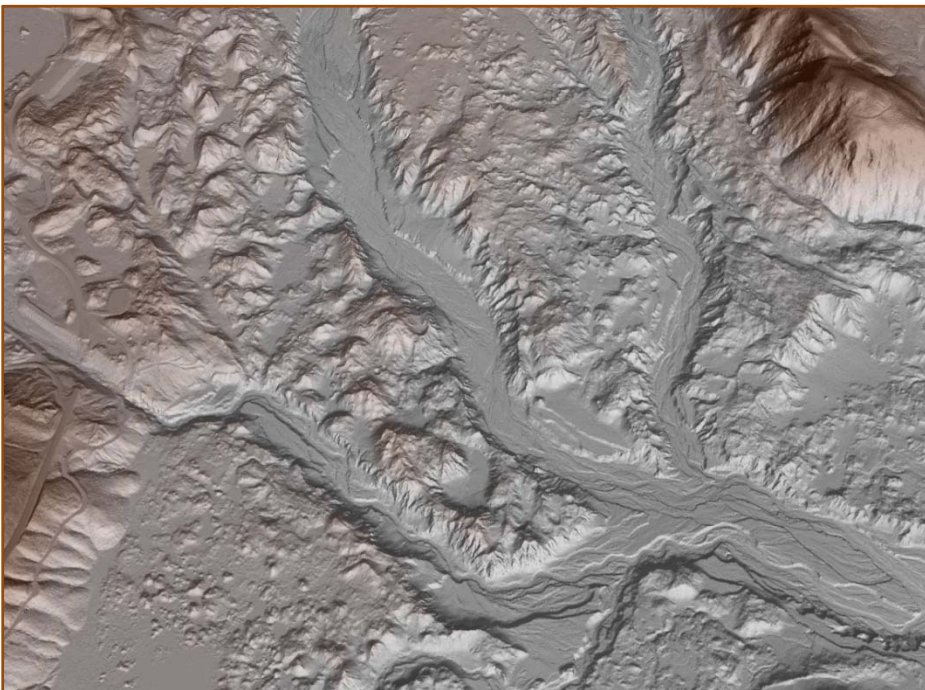
\*Note: Delineation based on 1/100<sup>th</sup> of a full 7.5-minute USGS Quad (.075-minutes). Larger delineations, such as 1/64<sup>th</sup> USGS Quads, resulted in unmanageable file sizes due to high data density.

Figure 9. Quadrangle naming convention for 1/100th of a 7.5-minute USGS Quad.



## 7. Selected Images

*Figure 10. 3D view looking South at the confluence of Coldwater (foreground) and Castle (background) Creeks with the Toutle River (top image is derived from highest-hit LiDAR points, and the bottom image is derived from ground-classified LiDAR points).*



*Figure 11. 3D views looking east northeast (slightly different vantage points) upstream along the Toutle River at the old Toutle Dam (center right) and debris dam site (upper center) along Hoffstadt Creek (top image is derived from ground-classified LiDAR points, and the bottom image is derived from highest-hit LiDAR points).*

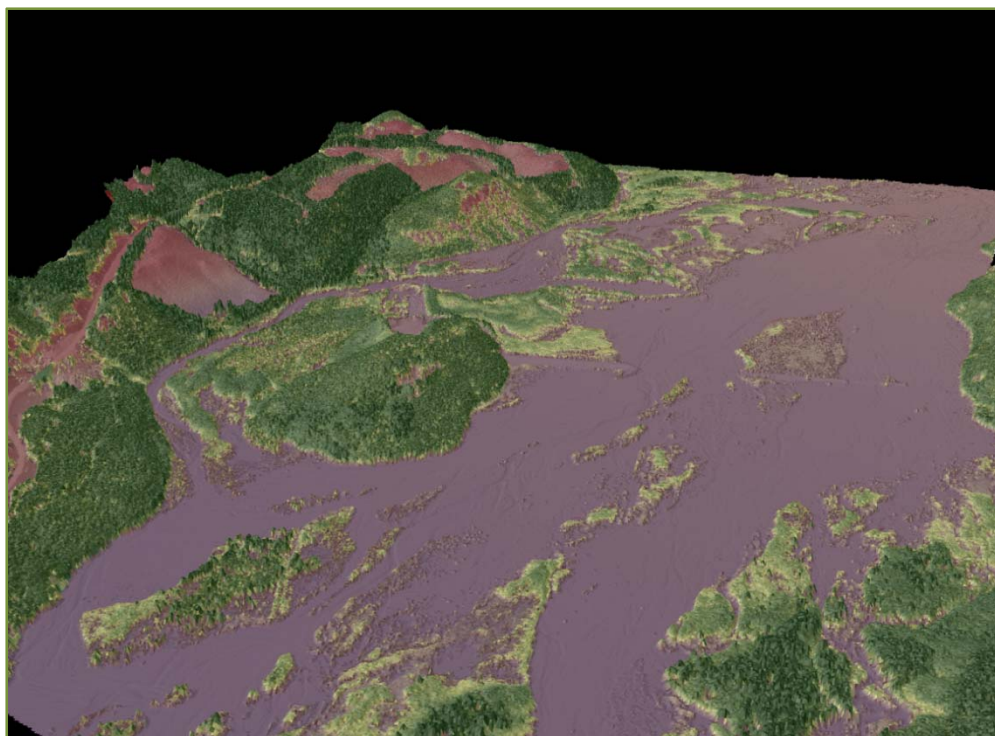
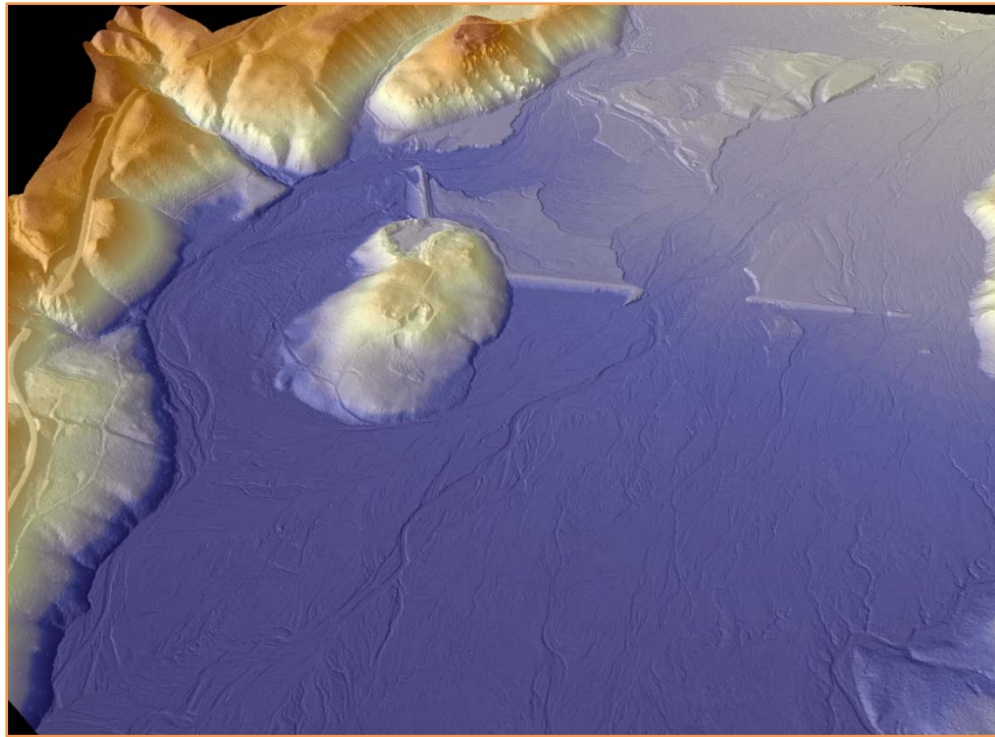


*Figure 12. LiDAR derived point cloud image colored by elevation textured by intensity. Image is an upstream view of the Toutle River at the old Toutle Dam site, with Hoffstadt Creek in the background.*

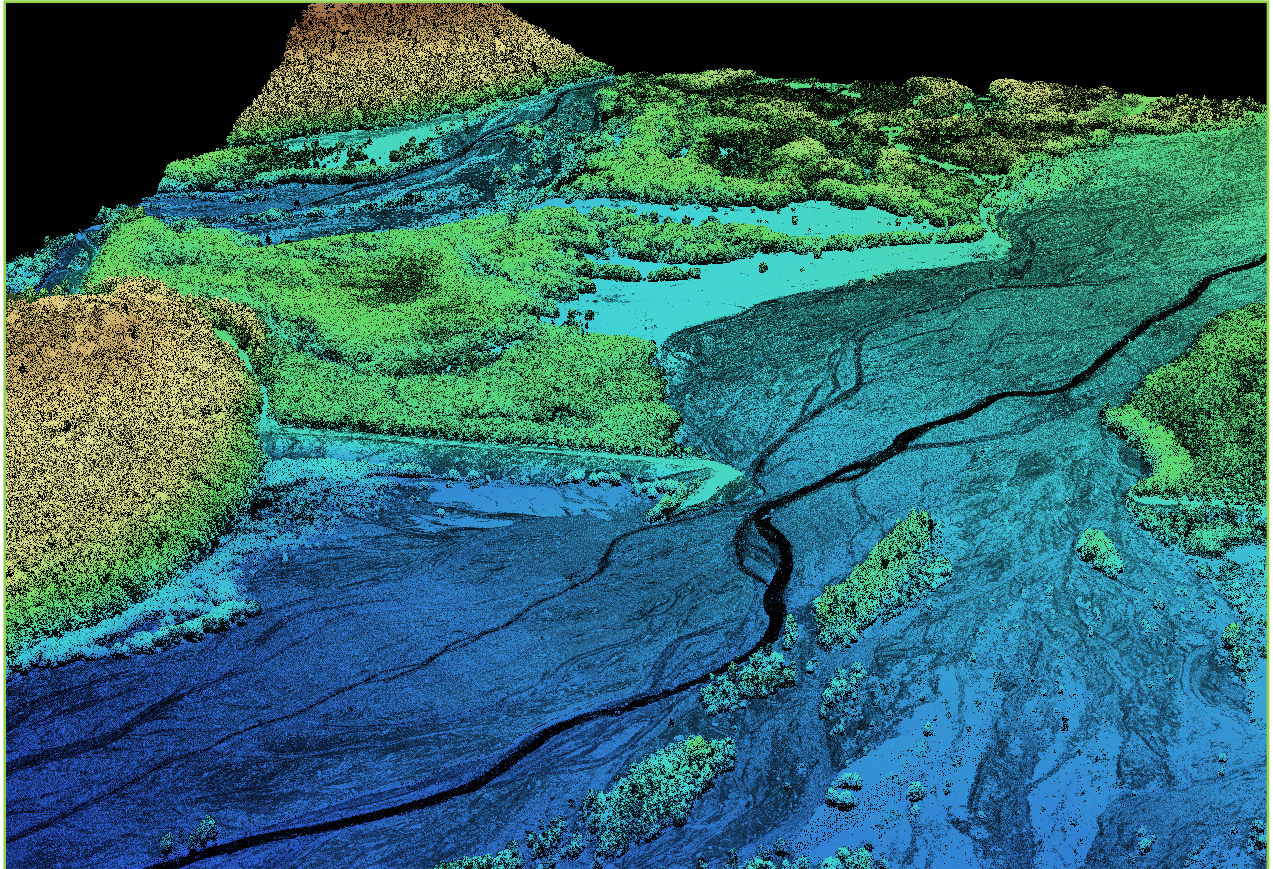


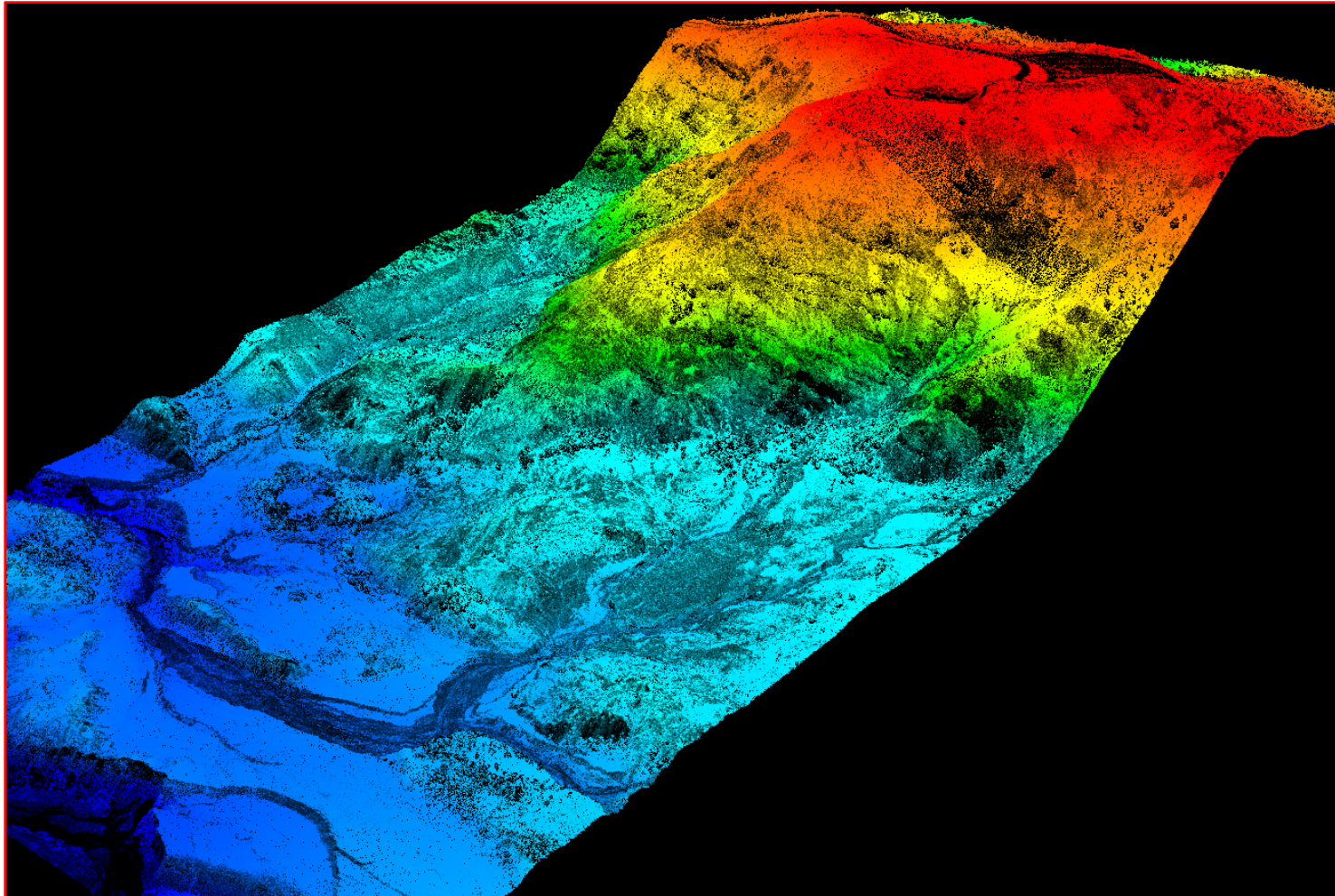
*Figure 13. 3D view looking south into the crater of Mt St Helens (image is derived from ground-classified LiDAR points).*



*Figure 14. Image is an overhead view of the southwestern shore of Spirit Lake, the pumice plain, and hummocks at the base of the Spillover Saddle of Johnson Ridge (clockwise starting in upper right). Image is derived from NAIP (National Agricultural Imagery Program) overlaid on LiDAR highest hit elevation model.*



*Figure 15. LiDAR derived point cloud images of Johnson Ridge Observatory colored by elevation and textured by intensity. View is to the northwest, with the observatory sitting above the Toutle River and blast zone of Mt St Helens.*





## 8. Glossary

**1-sigma ( $\sigma$ ) Absolute Deviation:** Value for which the data are within one standard deviation (approximately 68<sup>th</sup> percentile) of a normally distributed data set.

**2-sigma ( $\sigma$ ) Absolute Deviation:** Value for which the data are within two standard deviations (approximately 95<sup>th</sup> percentile) of a normally distributed data set.

**Root Mean Square Error (RMSE):** A statistic used to approximate the difference between real-world points and the LiDAR points. It is calculated by squaring all the values, then taking the average of the squares and taking the square root of the average.

**Pulse Rate (PR):** The rate at which laser pulses are emitted from the sensor; typically measured as thousands of pulses per second (kHz).

**Pulse Returns:** For every laser pulse emitted, the Leica ALS 50 Phase II system can record *up to four* wave forms reflected back to the sensor. Portions of the wave form that return earliest are the highest element in multi-tiered surfaces such as vegetation. Portions of the wave form that return last are the lowest element in multi-tiered surfaces.

**Accuracy:** The statistical comparison between known (surveyed) points and laser points.

Typically measured as the standard deviation ( $\sigma$ ) and root mean square error (RMSE).

**Intensity Values:** The peak power ratio of the laser return to the emitted laser. It is a function of surface reflectivity.

**Data Density:** A common measure of LiDAR resolution, measured as points per square meter.

**Spot Spacing:** Also a measure of LiDAR resolution, measured as the average distance between laser points.

**Nadir:** A single point or locus of points on the surface of the earth directly below a sensor as it progresses along its flight line.

**Scan Angle:** The angle from nadir to the edge of the scan, measured in degrees. Laser point accuracy typically decreases as scan angles increase.

**Overlap:** The area shared between flight lines, typically measured in percents; 100% overlap is essential to ensure complete coverage and reduce laser shadows.

**DTM / DEM:** These often-interchanged terms refer to models made from laser points. The digital elevation model (DEM) refers to all surfaces, including bare ground and vegetation, while the digital terrain model (DTM) refers only to those points classified as ground.

**Real-Time Kinematic (RTK) Survey:** GPS surveying is conducted with a GPS base station deployed over a known monument with a radio connection to a GPS rover. Both the base station and rover receive differential GPS data and the baseline correction is solved between the two. This type of ground survey is accurate to 1.5 cm or less.

## 9. Citations

Soininen, A. 2004. TerraScan User's Guide. TerraSolid.

## Appendix A

LiDAR accuracy error sources and solutions:

Type of Error	Source	Post Processing Solution
GPS (Static/Kinematic)	Long Base Lines	None
	Poor Satellite Constellation	None
	Poor Antenna Visibility	Reduce Visibility Mask
Relative Accuracy	Poor System Calibration	Recalibrate IMU and sensor offsets/settings
	Inaccurate System	None
Laser Noise	Poor Laser Timing	None
	Poor Laser Reception	None
	Poor Laser Power	None
	Irregular Laser Shape	None

Operational measures taken to improve relative accuracy:

Low Flight Altitude: Terrain following is employed to maintain a constant above ground level (AGL). Laser horizontal errors are a function of flight altitude above ground (i.e.,  $\sim 1/3000^{\text{th}}$  AGL flight altitude).

Focus Laser Power at narrow beam footprint: A laser return must be received by the system above a power threshold to accurately record a measurement. The strength of the laser return is a function of laser emission power, laser footprint, flight altitude and the reflectivity of the target. While surface reflectivity cannot be controlled, laser power can be increased and low flight altitudes can be maintained.

Reduced Scan Angle: Edge-of-scan data can become inaccurate. The scan angle was reduced to a maximum of  $\pm 14^{\circ}$  from nadir, creating a narrow swath width and greatly reducing laser shadows from trees and buildings.

Quality GPS: Flights took place during optimal GPS conditions (e.g., 6 or more satellites and PDOP [Position Dilution of Precision] less than 3.0). Before each flight, the PDOP was determined for the survey day. During all flight times, a dual frequency DGPS base station recording at 1-second epochs was utilized and a maximum baseline length between the aircraft and the control points was less than 19 km (11.5 miles) at all times.

Ground Survey: Ground survey point accuracy (i.e.  $<1.5$  cm RMSE) occurs during optimal PDOP ranges and targets a minimal baseline distance of 4 miles between GPS rover and base. Robust statistics are, in part, a function of sample size (n) and distribution. Ground survey RTK points are distributed to the extent possible throughout multiple flight lines and across the survey area.

50% Side-Lap (100% Overlap): Overlapping areas are optimized for relative accuracy testing. Laser shadowing is minimized to help increase target acquisition from multiple scan angles. Ideally, with a 50% side-lap, the most nadir portion of one flight line coincides with the edge (least nadir) portion of overlapping flight lines. A minimum of 50% side-lap with terrain-followed acquisition prevents data gaps.

Opposing Flight Lines: All overlapping flight lines are opposing. Pitch, roll and heading errors are amplified by a factor of two relative to the adjacent flight line(s), making misalignments easier to detect and resolve.

